THE JOURNAL OF PHYSICAL CHEMISTRY C

ARTICLE

pubs.acs.org/JPCC

# Molecular Dynamics Study of Crystalline Molecular Gyroscopes

Alexey V. Akimov and Anatoly B. Kolomeisky*

Department of Chemistry, Rice University, Houston, Texas 77005-1892, United States

Supporting Information

**ABSTRACT:** In recent years molecular rotors have attracted the attention of many research groups for possible applications as new nanoscale devices and materials with controlled chemical, physical, and mechanical properties. One of the most unique systems with molecular rotations is amphidynamic molecular crystals, also known as crystalline molecular gyroscopes. This system can be viewed as a solid-state assembly of molecules that cannot move translationally but show internal rotations. Recent experiments on amphidynamic crystals indicate importance of rotational symmetry for describing their dynamics. However, mechanisms and rotational dynamic properties of molecular gyroscopes are still not well understood. We present here a theoretical investigation of amphidynamic crystals by utilizing extensive rigid-body molecular dynamics simulations and simple phenomenological arguments. Theoretical analysis suggests that intramolecular interactions within stator and rotator segments of molecular rotors as well as their flexibility strongly affect their crystal packing, energies and rotational behavior. Our quantitative predictions for dynamic properties agree well with available experimental results.

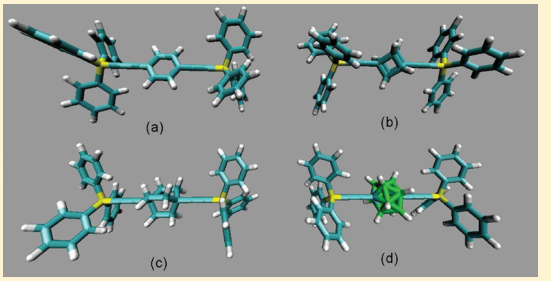




## 1. INTRODUCTION

Molecular machines and rotors are important functional components in all living organisms, playing critical roles in processes such as muscle contraction, cell division, motility, supporting cellular metabolism, vesicle and neuronal transport, as well as signaling and energy processing in cellular membranes.[1−7] High efficiency, flexibility, and robustness of biological nanomachines have stimulated significant experimental efforts to develop artificial molecular devices with potentially wide applications in nanotechnology, material science, and medicine.[8−21] Although many synthetic successes in this area have been reported, direct application of molecular motors and rotors in technology is still far away from the practical realization mainly because fundamental mechanisms of functioning of such systems are not well understood yet.[22]

One of the most promising directions in creating artificial molecular machines has been investigations of molecular rotors systems. Different systems that include molecular rotors working in solutions,[23−25] in liquid crystals,[26] on surfaces,[20,27−35] and in solid-state medium[36−43] have been reported in various experimental studies. These works have stimulated multiple theoretical investigations of mechanisms and properties of molecular rotors.[27,44−50] These studies allowed researchers to understand better the dynamics of many molecular rotors at the single-molecule level. However, many fundamental questions concerning microscopic mechanisms of functioning of such systems remain unanswered.

A new class of molecular rotors functioning in solid-state environment has been developed recently.[36−42] These materials, known as amphidynamic crystals (also called molecular gyroscopes), have been created synthetically by designing systems where strong translational interactions are uncoupled from internal rotational motions.[37] Thermally activated internal rotations in these solid-state molecular systems have been confirmed via temperature-dependent nuclear magnetic resonance (NMR) dynamic analysis.[51,52] In another study, it was argued that higher symmetry order to the rotator segment must lead to lower rotational barriers.[36] However, analysis of experimental observations indicates that symmetry alone can only partially explain some dynamic features of molecular rotations. In this paper, we present a theoretical investigation of amphidynamic crystals concentrating on the role of intramolecular interactions, vibrations, coupling, and flexibility of different segments. Our goal here is to develop a simple theoretical approach that would combine minimalist computational method with phenomenological arguments in order to get qualitative understanding of physical-chemical mechanisms of underlying phenomena.

## 2. METHODS

Our theoretical approach is based on performing and analyzing extensive molecular dynamics (MD) computer simulations for different amphidynamic crystals at different conditions. In particular, we utilized the rigid-body MD simulations method[53−56] that have been recently developed and successfully applied for various molecular motors and rotors systems such as carborane-wheeled and fullerene-wheeled nanocars on gold surfaces[57,58] and rotational dynamics of thioethers and ferrocene derivatives.[47,48] The

**Received:** March 1, 2011
**Revised:** June 1, 2011
**Published:** June 13, 2011

  

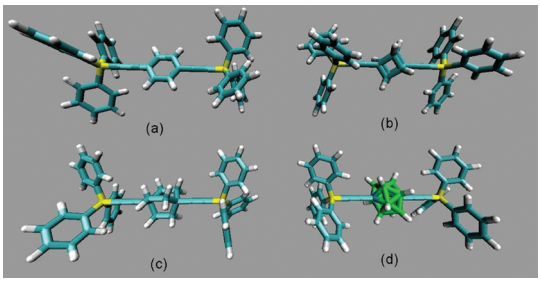


**Figure 1.** Molecular gyroscopes studied in this work. (a) Phe, (b) Cub, (c) BCO, and (d) Carbor.

method considers the studied molecules as coupled rigid segments while still accounting explicitly for all interatomic pairwise interactions. It allows speeding up computations significantly by neglecting some degrees of freedom that are less relevant for the overall dynamics. In addition, the problem of designing a proper coarse-grained potential is avoided here. Details of this computational method are available elsewhere.[47,48,57,58]

Specifically, we have studied four crystalline molecular rotor systems as shown in Figure 1. All these amphidynamic crystals have been investigated earlier experimentally,[36,42] so we can directly test our theoretical predictions. Each of these gyroscopes have a similar organic group (triphenylsilyl) at the ends that play the role of a stator and different central rotating groups, namely, phenylene, bicyclo[2,2,2]octanylidene, cubanylidene, and carboranylidene. For convenience, they are labeled as Phe, BCO, Cub, and Carbor, respectively; see Figure 1.

**2.1. Simulation Details.** Our MD computer simulations have been performed utilizing isothermal−isobaric conditions (NPT ensemble). Although we started with already developed algorithms,[53,54] several problems and issues in each of them have been found. As a result, an alternative approach was implemented (see the discussion in the Supporting Information). For each type of the molecular gyroscope a minimal system size of 4 molecules has been considered. To avoid boundary effects periodic boundary conditions (PBC) have been imposed on each system with a smooth cutoff described by van der Waals interactions with parameters $R_{on}$ = 8.0 Å and $R_{off}$ = 12.0 Å. A time-saving Verlet list technique for the case of NPT ensemble has been derived (see details of the derivation in the Supporting Information) and implemented leading to 2−4 times the acceleration over the standard approach that does not use the Verlet list.

The pressure of 1 atm has been maintained in all simulations, and a barostat frequency 0.002 $fs^{-1}$ has been used. The temperature was maintained by two Nose−Hoover chain thermostats[59,60] (of length 1 each) coupled to the barostat particle and atoms, respectively. The thermostats frequencies were 0.02 $fs^{-1}$ each. The integration time step for most types of MD simulations was taken to be 1 fs.

We obtained 5 independent trajectories for each molecular gyroscope and for each of the temperatures considered. The trajectory length was 1.1 ns, and the first 0.1 ns has been considered as an equilibration period that did not enter dynamic properties calculations, while the last 1.0 ns has been viewed as the production run to be used for calculations of observed quantities. One of such quantities is the rotational diffusion coefficient calculated as described in detail in our earlier work.[48]

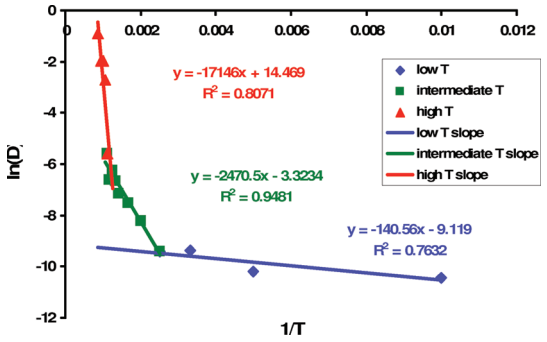


**Figure 2.** Typical rotational diffusion constants of molecular gyroscopes as a function of temperature.

Such an approach takes into account the direction of the rotation which is essential for this kind of calculations.

The rotational diffusion coefficient was estimated at different temperatures using the following procedure.[48] At each output time we calculated the rotation angle of the rotator around the axis, connecting the centers of the stators (Si−Si vector). By comparison of the current orientation with the previous one the decision was made in which direction the rotator has rotated for that period of time. This information has been used to evaluate the activation barriers for rotation of different species and the corresponding pre-exponential factors utilizing simple Arrhenius-like equation

$$D_{rot} = D_0 e^{-E_a/k_B T} \quad (1)$$

Since each simulation cell contained 4 molecules (i.e., 4 molecular rotors) moving relatively independent of each other, the actual amount of collected data for calculations of rotational properties was 4 times bigger (20 trajectories), which we believe was enough for obtaining reasonable sampling quality. As a force field to describe interatomic interactions in our MD simulations we have utilized a universal force field (UFF)[55] that contains parameters for most of the elements in the periodic system including those for silicon that is absent in many other force fields. It is known that UFF is inaccurate for describing dynamics of biological systems. However, it was shown that this force field was successful in many applications such as analyzing diffusion and transport through metal−organic materials,[62] studying phase transitions of ethylene glycol in zeolites,[63] and investigations of molecular packing in organic polymers.[64] Thus UFF provides a simple minimalist computational tool for studying artificial molecular motors and rotors, and this is the main reason we utilize it here for studying rotations in amphidynamic crystals.

**2.2. Temperature Range.** Analysis of all trajectories in MD simulations suggests that there are three temperature regimes for investigated amphidynamic crystals as illustrated in Figure 2. At low temperatures (up to 300 K) the dynamics is very slow and molecular rotors do not have enough time to sample all relevant configurations during the time of trajectories. Each molecule does not rotate but mostly fluctuates around the local minimum position. As a result, calculated energy barriers in this regime are very low since they describe mostly local dynamics when the rotor does not make complete turns. Effectively, the low-temperature regime is defined where the rotational diffusion occurs with a time constant greater than 1 ns. At higher temperatures (300−800 K) rotors are able to turn around many times, and good statistics on rotational dynamics

**Table 1. Comparison of the Calculated Properties of Rotors Depending on the Simulation Time**

| | $E_a$, kcal/mol | | | pre-exponent, $s^{-1}$ | | |
|---|---|---|---|---|---|---|
| rotor | experiment | short | long | experiment | short | long |
| Phe | $8.5 \pm 2.5$ | $8.0 \pm 0.8$ | $6.8 \pm 1.1$ | $1.1 \times 10^{13}$ | $1.6 \times 10^{12}$ | $0.74 \times 10^{12}$ |
| BCO | $3.5 \pm 0.2$ | $3.7 \pm 0.3$ | $3.8 \pm 2.2$ | $3.6 \times 10^{10}$ | $3.3 \times 10^{11}$ | $2.8 \times 10^{11}$ |
| Cub | $12.6 \pm 2.5$ | $6.6 \pm 0.9$ | $7.2 \pm 1.6$ | $9.6 \times 10^{11}$ | $1.1 \times 10^{12}$ | $1.0 \times 10^{12}$ |
| Carbor | $3.0 \pm 0.1$ | $5.0 \pm 0.7$ | $4.1 \pm 1.2$ | $6.4 \times 10^{10}$ | $2.0 \times 10^{11}$ | $8.2 \times 10^{10}$ |

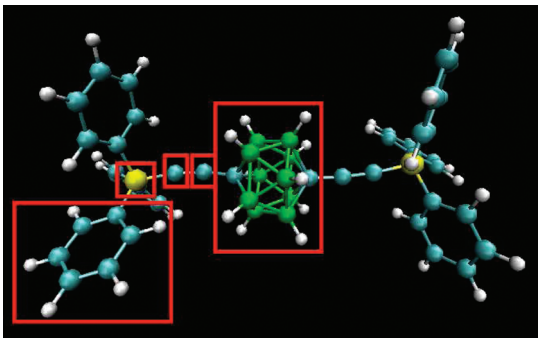

**Figure 3.** The rigid-body representation of the unit cell of Carbor amphidynamic crystals.

**Table 2. Rotational Activation Energies Calculated Using the Rigid-Body and All-Atomic MD Simulations and the Experimentally Obtained Values**

| rotor | rigid-body, kcal/mol | all-atomic, kcal/mol | experimental, kcal/mol |
|---|---|---|---|
| Phe | $8.0 \pm 0.7$ | $8.2 \pm 0.4$ | $8.5 \pm 2.5$ |
| BCO | $4.9 \pm 0.5$ | $5.3 \pm 0.4$ | $3.5 \pm 0.2$ |
| Cub | $6.3 \pm 0.9$ | | $12.6 \pm 2.5$ |
| Carbor | $4.9 \pm 0.4$ | | $3.0 \pm 0.1$ |

can be obtained. Finally, at very high temperatures (>800K) the system starts to melt, sublimate, and disintegrate into pieces. Thus, only intermediate temperature regime provides the most realistic description of the rotational dynamics. All calculations have been performed utilizing these intermediate temperatures.

**2.3. Trajectrory Length.** It is important to note that because the number of atoms in each simulation cell is around 400 and because of periodic boundary conditions we utilized 124 replicas (2 shells) of the original cell for computations. As a result, several millions of interactions must be computed in each MD step to fully describe the system. It limits the length of reliable trajectories that could be obtained using this method. However, it still allows us to analyze rotational dynamics of solid-state molecular rotors at some temperatures.

To access the importance of the simulation time on the calculated quantities we performed longer simulations (~4 ns) by using larger integration time step of 2.5 fs, 1 shell of periodic boundary conditions replicas (i.e., 26 additional cells), and smaller cutoff and Verlet list radii. The calculated dynamic properties obtained from these longer trajectories have been found to be statistically indistinguishable from shorter trajectories, although error bars increased (see Table 1.).

**Table 3. Pre-Exponential Factors for Rotational Speeds Calculated Using Rigid-Body and All-Atomic MD Simulations and the Experimentally Obtained Values**

| rotor | rigid-body, $s^{-1}$ | all-atomic, $s^{-1}$ | experimental, $s^{-1}$ |
|---|---|---|---|
| Phe | $1.7 \times 10^{12}$ | $3.1 \times 10^{12}$ | $1.1 \times 10^{13}$ |
| BCO | $9.1 \times 10^{11}$ | $1.6 \times 10^{12}$ | $3.6 \times 10^{10}$ |
| Cub | $7.6 \times 10^{11}$ | | $9.63 \times 10^{11}$ |
| Carbor | $1.9 \times 10^{11}$ | | $6.4 \times 10^{10}$ |

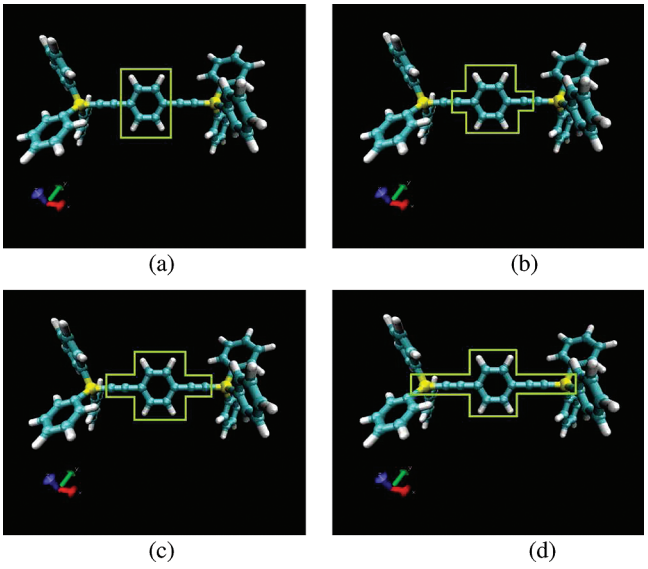


**Figure 4.** Various coarse-grain representations of the rotator part in Phe molecular gyroscope. These representations are labeled as: (a) Flex; (b) Flex1; (c) Flex2; (d) rod.

The increased error bars might be the consequence of the bigger integration time step. Since the number of time steps between the measurements of rotors orientation was the same as for short trajectories, the increase of the time step raises the time interval between such measurements, and it might result in bigger uncertainty of such measurements. Moreover, since the integration error becomes larger with the increase of the time step, the measured quantities could also be affected accordingly. On the basis of these studies we decided to use shorter but more reliable trajectories to analyze the dynamics of solid-state rotors.

## 3. RESULTS AND DISCUSSION

**3.1. All-Atomic vs Rigid-Body Simulations.** The rigid-body MD method is an approximate computational approach that neglects contribution from many degrees of freedom. To

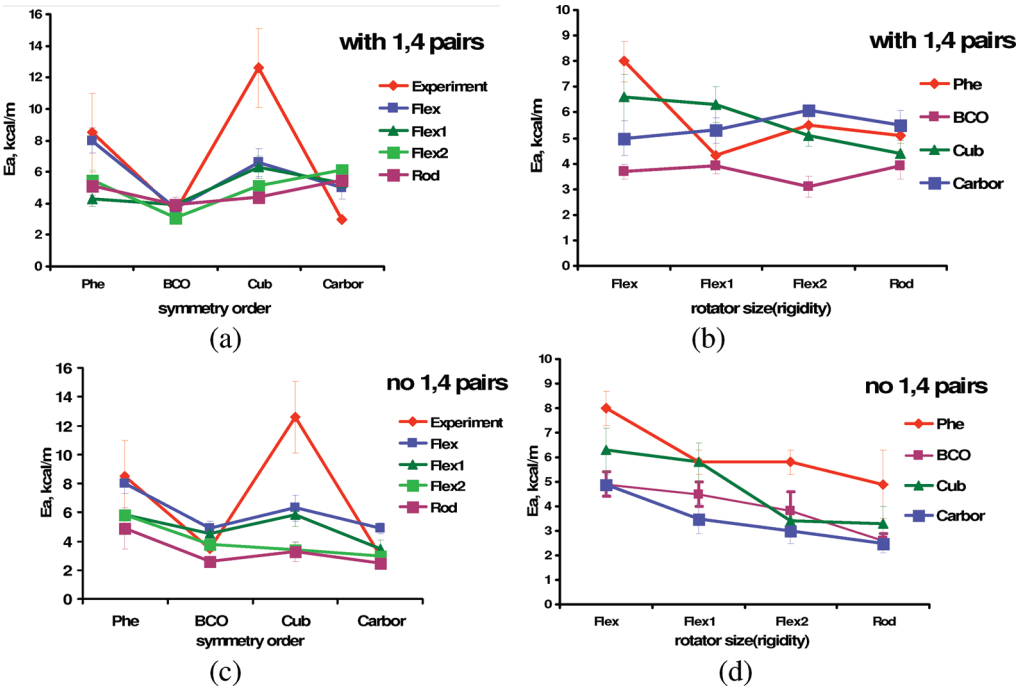


**Figure 5.** Rotational activation energies for different molecular rotors as a function of the symmetry (type of the rotator): (a) with 1,4 pair interactions; (c) without 1,4 pair interactions. Rotational activation energies for different molecular rotors as a function of flexibility: (b) with 1,4 pair interactions; (d) without 1,4 pair interactions.

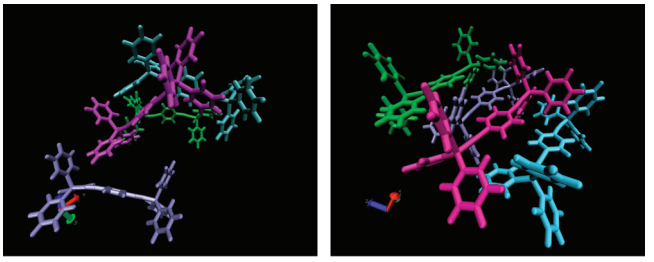


**Figure 6.** Packing of Phe molecular gyroscopes in the simulation cell at 600 K (a) without 1,4 pair interactions (disordered) and (b) with 1,4 pair interactions (ordered).

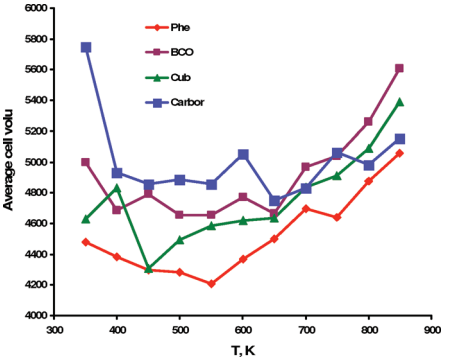


**Figure 7.** Average cell volumes for different molecular gyroscopes (in the most flexible representation) at different temperatures with 1,4 pair interactions.

test the applicability of this technique for molecular gyroscopes we performed all-atomic computer simulations for Phe and BCO systems, which have smallest rotator groups (see Figure 1), and compared them with rigid-body MD simulations. In our approximate computer simulations each molecule has been considered having 13 rigid fragments: rotator group, 6 phenyl groups in the stator part, 2 silicon atom, and 4 carbon atoms (in sp hybridization). Typical representation of the molecular gyroscope in terms of rigid segments is outlined in Figure 3 for Carbor system.

For the other two systems (Cub and Carbor) that have more complex rotator groups, only rigid-body computer simulations have been done. In this case, strong intramolecular repulsions would require very small integration time steps so only very short trajectories could be obtained. Then meaningful description of rotational dynamics cannot be obtained.

Rotational activation barriers and pre-exponential factors for molecular gyroscopes calculated utilizing all-atomic simulations and the rigid-body MD method are summarized in Tables 2 and 3. In addition, theoretical predictions are compared with experimental results obtained in temperature-dependent dynamic NMR measurements.[36] One can clearly see that our approximate method describes rotational dynamics of molecular gyroscopes as well as the more advanced MD simulation approach that fully accounts for all interatomic interactions. The agreement with experimental data is excellent for Phe systems, and it is reasonable for other molecular gyroscopes. The largest error is for Cub crystals where the rigid-body MD simulations underestimate significantly the rotational speed. However, it should be noted that our theoretical calculations reproduce the nonmonotonous trend in activation barriers as a function of rotator symmetry found in experiments.[36]

**3.2. Effects of Flexibility.** The rotational dynamics of molecular gyroscopes might depend on many factors such as size and


dx.doi.org/10.1021/jp201981v |J. Phys. Chem. C 2011, 115, 13584–13591

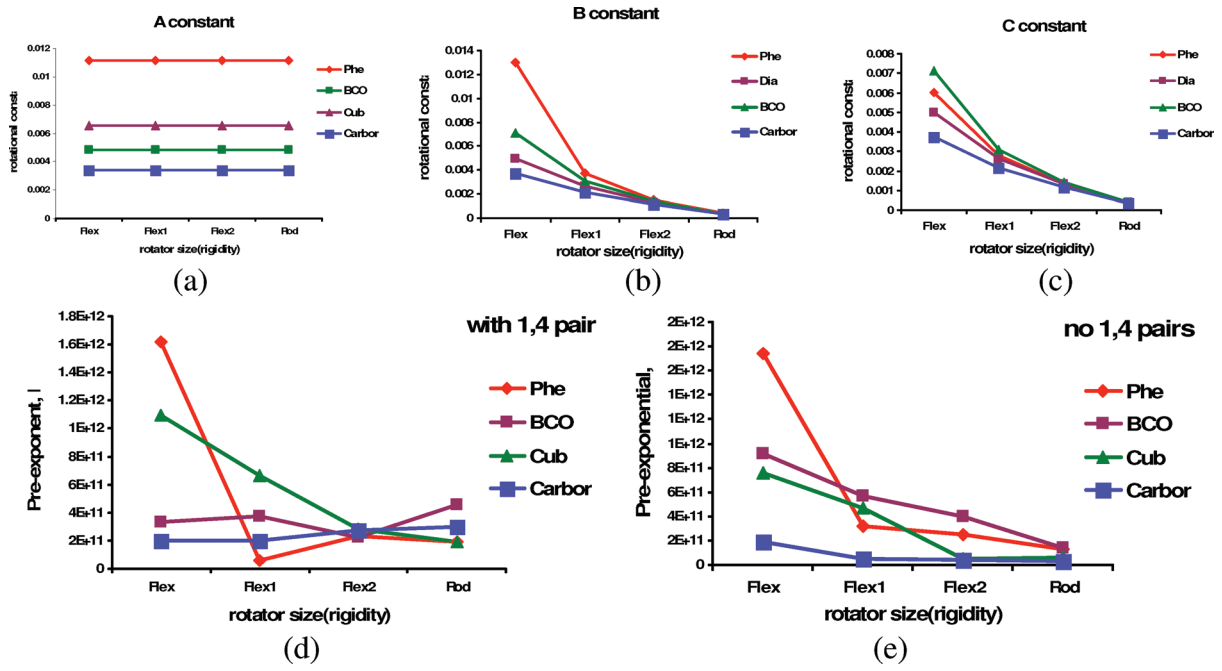


**Figure 8.** (a−c) Rotational constants (A, B, C) for different molecular gyroscopes. The pre-exponential factors for rotation obtained from MD simulations of rotors with a different size (rigidity) of the rotator and for different overall flexibilities of the molecule (d) with 1,4-pair interactions and (e) without 1,4-pair interactions.

structure of the rotors and vibrational coupling between rotator and stator groups. Our rigid-body MD method allows us to investigate these effects in detail by modifying the size of the rigid segment in the rotator group. We have considered 4 different types of coarse-graining representation of molecular gyroscopes as shown in Figure 4 for the Phe system. They differ by the size of the central rotator rigid segment. The rigid segment is the smallest in Figure 4a and the largest in Figure 4d.

We also studied the effect of molecular flexibility in stator and rotator segments by taking into account or neglecting nonbonded interactions in 1,4 pairs of terminal atoms of each dihedral. Rotational energy barriers as a function of molecular symmetry and flexibility are summarized in Figure 5. Additional results may be found in the Supporting Information.

Our results indicate that molecular symmetry does not fully determine rotational barriers for amphidynamic crystals (parts a and c of Figure 5), in agreement with current experiments. Moreover, molecular gyroscopes generally rotate more freely with increasing rigidity of the rotator segment: see parts b and d of Figure 5. This trend is especially clear for the case where 1,4 interactions are neglected. At the same time, including 1,4 interactions decrease coupling of rotational dynamics with the rigidity of the central segment.

Analysis of trajectories obtained in MD simulations (see movies in the Supporting Information) point out to the importance of 1,4 interactions. Specifically, when such interactions are included the observed molecule packing is much more ordered, and it becomes very similar to what is observed in experiments. When 1,4 interactions are not taken into account the resulting structures are much more disordered and the molecules in the unit cell are not aligned with each other. It is interesting to note that increasing the rigidity of the central part also favors less ordered solid-state structures.

**3.3. Activation Energies.** To understand rotational dynamics of molecular gyroscopes it is convenient to introduce a concept of a "free volume" for the rotator segment. This may be defined as the volume where the rotator is enclosed by the surrounding groups and where it might move more or less freely. The free volume is determined by a combination of interactions with other atoms and molecules. When this volume is small, the rotator interacts strongly with its neighbors, i.e., it feels the steric hindrance leading to high activation barriers and high attempt frequency. This is the case for Phe amphidynamic crystals. On the contrary, when the rotator has a large free volume the rotational speed is high because of lower activation barriers (although attempt frequencies might also be low). This situation describes well the BCO and the Carbor amphidynamic crystals. The free volume is affected by many factors that include flexibility of the stator and rotator segments and the size of the rotator.

Higher flexibility of the rotor (both stator and rotator segments) allows molecules to find the most energetically favorable packing configurations and thus minimize the free volume of rotators. It turns out that the packing configuration is mostly determined by the stator part. It can be seen by comparing packing structures for conditions with and without 1,4 pair interactions as illustrated in Figure 6. Neglecting these interactions allows phenyl groups to be very mobile. Corresponding MD trajectories show fast rotations of these fragments resulting in increased disorder in the system—the molecules do not pack as observed in experiments (Figure 6a).[36]

When the 1,4 pair interactions are accounted for, the rigidity of the $-C(Ph)_3$ group increases, and that ultimately leads to the stabilization of the packing configuration where all molecules are aligned parallel to each other. Such packing configurations are very similar to what was observed in experiments (Figure 6b).[36] Decreased mobility of the phenyl groups (due to steric hindrance of other phenyl groups) in one stator fragment assists the

formation of specific lock-and-key interactions with the stator part of another rotor molecule. The specific stacking pattern in the crystal determines the maximal free volume of the rotator possible for given molecular gyroscope. At these conditions the size of the rotator part may become important. If the rotator segment volume is comparable to the maximal free volume of the rotator then there is no more possibility to change that volume, so the activation energies become independent of the flexibility of the rotator (Figure 5b for BCO and Carbor). However, for small rotator groups there is a possibility to decrease their free volume due to better packing possible for flexible groups. Thus, in this case we observe the situation similar to that presented for rotors without 1,4 pair interactions. Namely, as the flexibility of the rotator part increases the activation energies increase too.

To check our hypothesis about free volumes and the most efficient packing of the molecules we calculated the average simulation cell volumes for all rotors in a wide range of temperatures (Figure 7). One can clearly see that for the most of the temperature range the average volumes compares follow the following trend, $V_{Phe} < V_{Cub} < V_{BCO} \approx V_{Carbor}$. This sequence correlates well with the calculated rotational activation energies. Carbor and BCO are the fastest rotators, while Phe and Cub show much slower rotational dynamics: see Figure 5. Thus, the packing density and consequently the "free volume" of rotator are important factors determining rotational barriers.

**3.4. Pre-Exponential Factors.** Pre-exponential factors in rotational speeds, also known as attempt frequencies, are important parameters that characterize dynamics of molecular gyroscopes. They correspond to maximal rotational velocity that the rotator segment can achieve in the absence of any interactions. The maximal angular velocity of the object rotating with a given kinetic energy is determined by its inertia tensor. Thus there must be a correlation between the rotational constants (quantities inversely proportional to the principal moments of inertia) and the observed pre-exponential factors.

We calculated the rotational constants for rotators of different size (parts a−c of Figure 8), which were used in our MD simulations. The only constant which is relatively independent of the rotator size is A constant (Figure 8a). It describes the motion around the rotation axis. Other two rotational constants correspond to rotations around two other axes, orthogonal to the rotation axis and to each other.

Our MD calculations show that this correlation is indeed observed: see parts d and e of Figure 8 and Table S2 in the Supporting Information. As shown in Figure 8, increasing the size of the rigid rotator increases its moments of inertia and lowers the rotational constants. The same trend is observed for the attempt frequencies.

## 4. SUMMARY AND CONCLUSIONS

Rotational dynamics of molecular gyroscopes in amphidynamic crystals have been investigated theoretically by analyzing extensive numerical data obtained from rigid-body MD computer simulations. It was shown that our coarse-grained computational method performs as well as more precise all-atomic MD computer simulations. Obtained theoretical results are also found to be in a reasonable agreement with available experimental observations.

We analyzed existing methods to perform rigid-body MD simulations in the case of NPT ensemble and found some important aspects of implementations of the underlying algorithms needed some corrections. In particular, it was found that some of the expressions should be properly modified in order to be used in simulations of such kind. In addition, we reformulated existing automatic update of the Verlet list technique and extended it to the case of varying simulation cell. Such extension is necessary for correct and fast simulations in the NPT ensemble. Utilizing this computational method we achieved accelerations in calculations up to 4 times, depending on simulation parameters.

Our theoretical calculations show that rotational properties of molecular gyroscopes are determined by flexibility and size of the rotator group and by the strength of interactions in the stator segments. The following general picture of rotational dynamics for molecular gyroscopes is proposed. Strong interactions in the stator segments lead to ordered crystalline phases with specified free volume for rotations of the central group. In this case the dependence on the properties of the rotator is relatively small. When the stator is more flexible it introduces significant disorder, and in this case properties of the rotator groups are critical for the overall rotational dynamics. Comparing amphidynamic crystals with similar stator interactions and different rotator properties suggest that more flexible rotators have lower rotational speeds due to increasing interactions with the local environment. Longer and more rigid rotators have smaller activation barriers and smaller attempt frequencies. Our theoretical analysis suggests that rotational dynamics in solid-state systems might be controlled by adjusting molecular flexibility, interactions, and couplings in stator and rotator segments. It will be important to test these theoretical predictions in future experiments on amphidynamic crystals.

In addition, our theoretical method also supports recent experimental studies which suggested that rotational barriers are generally larger for less symmetric rotator groups. The fact that experimentally observed deviation from this rule for Cubanylidene rotator is also found in our simulations indicates that the presented theoretical approach probably correctly describes properties of solid-state rotors.

Although the presented theoretical approach is simple and physically intuitive, and it provides a good description of experimental observations in amphidynamic crystals; it is noted that several approximations and assumptions have been made in the developing of the model. Perhaps the weakest points of this method are the use of UFF force field and neglect of electrostatic interactions. It will be important to study these systems by utilizing other force fields and taking into account charges and polarizabilities of involved organic groups. Despite the approximate nature of the UFF force field it has been successfully applied in different molecular systems,[62−64] and it validates the application of this method in our approach. In addition, studied solid-state rotors did not contain polar groups suggesting that electrostatic effects might be not very important. Good agreement between calculated and experimentally measured activation energies and pre-exponential factors support this argument. The advantage of our theoretical method is that it provides a reasonably simple approach for understanding microscopic mechanisms of rotations, and it can be used as a starting point for development of nanodevices and new materials based on assemblies of molecular rotors.

## ■ ASSOCIATED CONTENT

**Supporting Information.** Derivations of the criteria used for automatic update of the Verlet list during MD simulations in

NPT ensemble and corrections for MD methodology used in other works; calculated activation energies and pre-exponential factors in digital form; animated movies of selected MD trajectories. This material is available free of charge via the Internet at http://pubs.acs.org.

## AUTHOR INFORMATION

**Corresponding Author**
*E-mail: tolya@rice.edu.

## ACKNOWLEDGMENT

Authors acknowledge support from the Welch Foundation (Grant C-1559) and from the U.S. National Science Foundation (Grant ECCS-0708765). This work was also supported in part by the Shared University Grid at Rice University funded by U.S. National Science Foundation under Grant EIA-0216467 and a partnership between Rice University, Sun Microsystems, and Sigma Solutions, Inc. A.B.K. also would like to thank M. A. Garcia-Garibay for useful comments and discussions.

## REFERENCES

(1) Lodish, H.; Zipursky, S. L.; Matsudaira, P.; Baltimore, D.; Darnell, J., *Molecular Cell Biologsy*, 4th ed.; W.H. Freeman and Company: New York, 2000.
(2) Bray, D. *Cell Movements: from molecules to motility*, 2nd ed.; Garland Publishing: New York, 2001.
(3) Howard, J., *Mechanics of Motor Proteins and the Cytoskeleton*; Sinauer Associates: Sunderland, MA, 2001.
(4) Schliwa, M.; Woehlke, G. *Nature* **2003**, *422*, 759.
(5) Kolomeisky, A.; Fisher, M. E. *Annu. Rev. Phys. Chem.* **2007**, *58*, 675.
(6) Balzani, V.; Gomez-Lopez, M.; Stoddart, J. F. *Acc. Chem. Res.* **1998**, *31*, 405–414.
(7) Kinbara, K.; Aida, T. *Chem. Rev.* **2005**, *105*, 1377.
(8) Xue, M.; Kabehie, S.; Stieg, A. Z.; Tkatchouk, E.; Benitez, D.; Goddard, W. A.; Zink, J. I.; Wang, K. L. *Electr. Dev. Lett., IEEE* **2010**, *31*, 1047–1049.
(9) Eelkema, R.; Pollard, M. M.; Vicario, J.; Katsonis, N.; Serrano Ramon, B.; Bastiaansen, C. W. M.; Broer, D. J.; Feringa, B. L. *Nature* **2006**, *440*, 163–163.
(10) Haidekker, M. A.; Theodorakis, E. A. *J. Biol. Eng.* **2010**, *4*, 11.
(11) Kuimova, M. K.; Yahioglu, G.; Levitt, J. A.; Suhling, K. *J. Am. Chem. Soc.* **2008**, *130*, 6672–6673.
(12) Stoddart, J. F. *Acc. Chem. Res.* **2001**, *34*, 410.
(13) Balzani, V.; Gomez-Lopez, M.; Stoddart, J. F. *Acc. Chem. Res.* **1998**, *31*, 405.
(14) Collin, J.; Dietrich-Buchecker, C.; Gaviña, P.; Jimenez-Molero, M. C.; Sauvage, J. *Acc. Chem. Res.* **2001**, *34*, 477.
(15) Amendola, V.; Fabbrizzi, L.; Mangano, C.; Pallavicini, P. *Acc. Chem. Res.* **2001**, *34*, 488.
(16) Shirai, Y.; Morin, J.; Sasaki, T.; Guerrero, J. M.; Tour, J. M. *Chem. Soc. Rev.* **2006**, *35*, 1043.
(17) Harada, A. *Acc. Chem. Res.* **2001**, *34*, 456.
(18) Browne, W. R.; Feringa, B. L. *Nature Nanotechnol.* **2006**, *1*, 25.
(19) Badjic, J. D. *Science* **2004**, *303*, 1845.
(20) Van Delden, R. A.; ter Wiel, M. K. J.; Pollard, M. M.; Vicario, J.; Koumura, N.; Feringa, B. L. *Nature* **2005**, *437*, 1337.
(21) Villagomez, C. J.; Sasaki, T.; Tour, J. M.; Grill, L. *J. Am. Chem. Soc.* **2010**, *132*, 16848.
(22) Michl, J.; Sykes, E. C. H. *ACS Nano* **2009**, *3*, 1042.
(23) Leigh, D. A.; Wong, J. K. Y.; Dehez, F.; Zerbetto, F. *Nature* **2003**, *424*, 174–179.
(24) Kelly, T. R.; De Silva, H.; Silva, R. A. *Nature* **1999**, *401*, 150–152.
(25) Koumura, N.; Zijlstra, R. W.; van Delden, R. A.; Harada, N.; Feringa, B. L. *Nature* **1999**, *401*, 152–155.
(26) Tabe, Y.; Yokoyama, H. *Nat. Mater.* **2003**, *2*, 806–809.
(27) Horinek, D.; Michl, J. *Proc. Natl. Acad. Sci. U.S.A.* **2005**, *102*, 14175.
(28) Magnera, T. F.; Michl, J. *Top. Curr. Chem.* **2005**, *262*, 63–97.
(29) Balzani, V.; Credi, A.; Venturi, M. *Chem. Phys. Chem.* **2008**, *9*, 202–220.
(30) Zhong, D.; Wedeking, K.; Chi, L.; Erker, G.; Fuchs, H. *Nano Lett.* **2009**, *9*, 4387–4391.
(31) Zheng, X.; Mulcahy, M. E.; Horinek, D.; Galeotti, F.; Magnera, T. F.; Michl, J. *J. Am. Chem. Soc.* **2004**, *126*, 4540–4542.
(32) Thibeault, D.; Auger, M.; Morin, J. F. *Eur. J. Org. Chem.* **2010**, *2010*, 3049–3067.
(33) Gao, L.; Du, S. X.; Gao, H. J. *Int. J. Mol. Sci.* **2010**, *11*, 656.
(34) Hai-Gang, Z.; Jin-Hai, M.; Qi, L.; Nan, J.; Hai-Tao, Z.; Hai-Ming, G.; Dong-Xia, S.; Hong-Jun, G. *Chin. Phys. B* **2010**, *19*, 018105.
(35) Jewell, A. D.; Tierney, H. L.; Baber, A. E.; Iski, E. V.; Laha, M. M.; Sykes, E. C. *J. Phys: Condens. Matter* **2010**, *22*, 264006.
(36) Karlen, S. D.; Reyes, H.; Taylor, R. E.; Khan, S. I.; Hawthorne, M. F.; Garcia-Garibay, M. A. *Proc. Natl. Acad. Sci. U.S.A.* **2010**, *107*, 14973.
(37) Garcia-Garibay, M. A. *Proc. Natl. Acad. Sci. U.S.A.* **2005**, *102*, 10771.
(38) Dominguez, Z.; Dang, H.; Strouse, M. J.; Garcia-Garibay, M. A. *J. Am. Chem. Soc.* **2002**, *124*, 2398.
(39) Dominguez, Z.; Khuong, T. V.; Dang, H.; Sanrame, C. N.; Nuñez, J. E.; Garcia-Garibay, M. A. *J. Am. Chem. Soc.* **2003**, *125*, 8827.
(40) Rodriguez-Molina, B.; Ochoa, M. E.; Farfán, N.; Santillan, R.; Garcia-Garibay, M. A. *J. Org. Chem.* **2009**, *74*, 8554.
(41) O'Brien, Z. J.; Karlen, S. D.; Khan, S.; Garcia-Garibay, M. A. *J. Org. Chem.* **2010**, *75*, 2482.
(42) Karlen, S. D.; Ortiz, R.; Chapman, O. L.; Garcia-Garibay, M. A. *J. Am. Chem. Soc.* **2005**, *127*, 6554.
(43) Comotti, A.; Bracco, S.; Valsesia, P.; Beretta, M.; Sozzani, P. *Ang. Chem. Int. Ed.* **2010**, *49*, 1760.
(44) Vacek, J.; Michl, J. *Adv. Funct. Mater.* **2007**, *17*, 730.
(45) Astumian, R. D. *Proc. Natl. Acad. Sci. U.S.A.* **2005**, *102*, 1843.
(46) Astumian, R. D. *Phys. Chem. Chem. Phys.* **2007**, *9*, 5067.
(47) Tierney, H. L.; Baber, A. E.; Sykes, E. C. H.; Akimov, A.; Kolomeisky, A. B. *J. Phys. Chem. C* **2009**, *113*, 10913.
(48) Akimov, A.; Kolomeisky, A. B. *J. Phys. Chem. C* **2011**, *115*, 125.
(49) Clarke, L. I.; Horinek, D.; Kottas, G. S.; Varaksa, N.; Magnera, T. F.; Hinderer, T. P.; Horansky, R. D.; Michl, J.; Price, J. C. *Nanotechnology* **2002**, *13*, 533.
(50) Jose, D.; Datta, A. *J. Phys. Chem. Lett.* **2010**, *1*, 1363.
(51) Khuong, T. A. V.; Zepeda, G.; Ruiz, R.; Kahn, S. I.; Garcia-Garibay, M. A. *Cryst. Growth Des.* **2004**, *4*, 15.
(52) Garcia-Garibay, M. A.; Godinez, C. E. *Cryst. Growth Des.* **2009**, *9*, 3124.
(53) Kamberaj, H.; Low, R. J.; Neal, M. P. *J. Chem. Phys.* **2005**, *122*, 224114.
(54) Ikeguchi, M. *J. Comput. Chem.* **2004**, *25*, 529–541.
(55) Dullweber, A.; Leimkuhler, B.; McLachlan, R. *J. Chem. Phys.* **1997**, *107*, 5840–5851.
(56) Miller, T. F.; Eleftheriou, M.; Pattnaik, P.; Ndirango, A.; Newns, D.; Martyna, G. J. *J. Chem. Phys.* **2002**, *116*, 8649.
(57) Akimov, A. V.; Nemukhin, A. V.; Moskovsky, A. A.; Kolomeisky, A. B.; Tour, J. M. *J. Chem. Theor. Comp.* **2008**, *4*, 652.
(58) Konyukhov, S. S.; Kupchenko, I. V.; Moskovsky, A. A.; Nemukhin, A. V.; Akimov, A. V.; Kolomeisky, A. B. *J. Chem. Theory Comput.* **2010**, *6*, 2581.
(59) Okumura, H.; Itoh, S. G.; Okamoto, Y. *J. Chem. Phys.* **2007**, *126*, 084103.
(60) Tuckerman, M. E.; Liu, Y.; Ciccotti, G.; Martyna, G. J. *J. Chem. Phys.* **2001**, *115*, 1678.

(61) Rappe, A. K.; Casewit, C. J.; Colwell, K. S.; Goddard Iii, W. A.; Skiff, W. M. *J. Am. Chem. Soc.* **1992**, *114*, 10024–10035.
(62) Skoulidas, A. I.; Sholl, D. S. *J. Phys. Chem. B* **2005**, *109*, 15760–15768.
(63) Huwe, A.; Kremer, F.; Behrens, P.; Schwieger, W. *Phys. Rev. Lett.* **1999**, *82*, 2338–2341.
(64) Chen, S. H.; Chou, H. L.; Su, A. C.; Chen, S. A. *Macromolecules* **2004**, *37*, 6833–6838.